Biochimica et Biophysica Acta 1844 (2014) 1784–1789

Contents lists available at ScienceDirect

Biochimica et Biophysica Acta

journal homepage: www.elsevier.com/locate/bbapap

An evolutionarily conserved alternate metal ligand is important for activity in α-isopropylmalate synthase from *Mycobacterium tuberculosis*☆

Patrick A. Frantom *, Yuliya Birman, Brittani N. Hays, Ashley K. Casey

Department of Chemistry, The University of Alabama, 250 Hackberry Lane, Tuscaloosa, AL 35406, USA

ARTICLE INFO

Article history:
Received 15 March 2014
Received in revised form 14 July 2014
Accepted 16 July 2014
Available online 23 July 2014

Keywords:
Isopropylmalate synthase
DRE-TIM metallolyase superfamily
Metalloenzyme
Enzyme catalysis

ABSTRACT

Members of the DRE-TIM metallolyase superfamily rely on an active-site divalent cation to catalyze various reactions involving the making and breaking of carbon–carbon bonds. While the identity of the metal varies, the binding site is well-conserved at the superfamily level with an aspartic acid and two histidine residues acting as ligands to the metal. Previous structural and bioinformatics results indicate that the metal can adopt an alternate architecture through the addition of an asparagine residue as a fourth ligand. This asparagine residue is strictly conserved in all members of the DRE-TIM metallolyase superfamily except fungal homocitrate synthase (HCS-lys) where it is replaced with isoleucine. The role of this additional metal ligand in α-isopropylmalate synthase from *Mycobacterium tuberculosis* (MtIPMS) has been investigated using site-directed mutagenesis. Substitution of the asparagine ligand with alanine or isoleucine results in inactive enzymes with respect to α-isopropylmalate formation. Control experiments suggest that the substitutions have not drastically affected the enzyme's structure indicating that the asparagine residue is essential for catalysis. Interestingly, all enzyme variants retained acetyl CoA hydrolysis activity in the absence of α-ketoisovalerate, similar to the wild-type enzyme. In contrast to the requirement of magnesium for α-isopropylmalate formation, hydrolytic activity could be inhibited by the addition of magnesium chloride in wild-type, D81E, and N321A MtIPMS, but not in the other variants studied. Attempts to rescue loss of activity in N321I MtIPMS by mimicking the fungal HCS active site through the D81E/N321I double variant were unsuccessful. This suggests epistatic constraints in evolution of function in IPMS and HCS-lys enzymes.

1. Introduction

Over the past decade, the identification and characterization of enzyme superfamilies have provided extraordinary insight into the evolution of enzyme function [1–3]. A superfamily represents a group of evolutionarily related enzymes that share a common mechanistic aspect in the stabilization of an intermediate enabled by conserved active site architecture [4]. Within a superfamily, subgroups of enzymes can be identified that catalyze diverse sets of chemical reactions often complicating functional predictions. Residues conserved throughout the superfamily can be implicated as critical to a catalytic step in the mechanism or required for structural stability. In contrast, residues conserved at the subgroup level are predicted to provide unique functionality to each subgroup such as differences in substrate selectivity and regulatory mechanisms.

The DRE-TIM metallolyase superfamily contains enzymes involved in making and breaking C–C bonds in various metabolic pathways across all three domains of life [5]. This superfamily includes the enzymes isopropylmalate synthase (IPMS[1]), 3-hydroxy-3-methylglutaryl-CoA lyase (HMG-CoA lyase), 2-hydroxy-4-ketovalerate aldolase, and pyruvate carboxylase, with each activity represented by a unique subgroup. Structurally these four enzymes share a TIM barrel catalytic domain and require a divalent cation for activity. The divalent metal is liganded by three well-conserved amino acids: an aspartic acid and two histidine residues in an HXH motif (pink structure, Fig. 1A). In most members, oxygen atoms from substrate and active site water molecules contribute the remaining ligands to the metal.

IPMS is a well-characterized member of the DRE-TIM metallolyase superfamily [6]. The enzyme catalyzes a Claisen-like condensation between α-ketoisovalerate (KIV) and acetyl-CoA (AcCoA) followed by hydrolysis of the isopropylmalyl-CoA intermediate resulting in isopropylmalate (IPM) and CoA (Scheme 1). This is the first step in the biosynthesis of L-leucine in archaea, bacteria, and some eukaryotes

Abbreviations: AcCoA, acetyl coenzyme A; CMS, citramalate synthase; HCS, homocitrate synthase; HMG-CoA lyase, 3-Hydroxy-3-methylglutaryl-CoA lyase; IPMS, α-Isopropylmalate synthase; KIV, α-Ketoisovalerate; MtIPMS, IPMS from *Mycobacterium tuberculosis*; ScHCS, homocitrate synthase from *Saccharomyces cerevisiae*

☆ This work was supported by The University of Alabama and NSF grant MCB-1254077 (P.A.F.)

* Corresponding author at: Department of Chemistry, The University of Alabama, Box 870336, Tuscaloosa, AL 35406, USA. Tel.: +1 205 348 8349; fax: +1 205 348 9104.
E-mail address: pfrantom@ua.edu (P.A. Frantom).

http://dx.doi.org/10.1016/j.bbapap.2014.07.013
1570-9639/

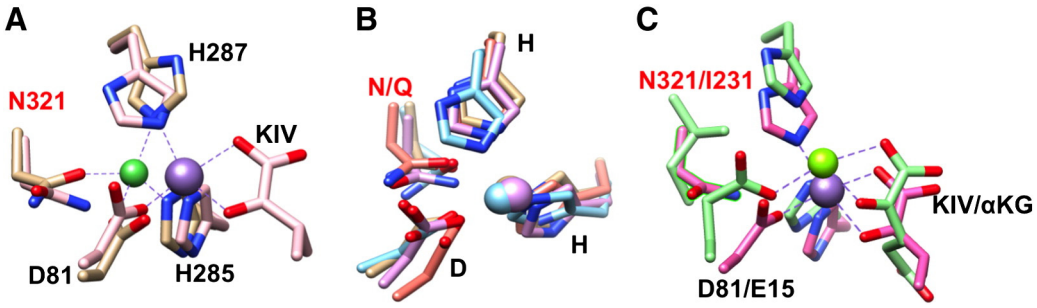

Fig. 1. A) Superposition of metal ion binding locations in MtIPMS. PDB files 3u6w (pink) and 3hpx (brown) were superimposed using Matchmaker program in Chimera. The purple sphere represents a Mn^{2+} ion from 3u6w, and the green sphere represents a Ni^{2+} ion from 3hpx. The additional metal ligand is labeled in red. B) Superposition of metal binding residues in the DRE-TIM metallolyase superfamily. Structures shown include citramalate synthase from *L. interrogans* (3bli, brown), HMG-CoA lyase from *H. sapiens* (3mp3, pink), 4-OH-2-oxovalerate aldolase from *Psuedomonas sp.* CF600 (1nmv, purple), and pyruvate carboxylase from *Rhizobium etli* (4jx5, cyan). Superposition was created using Chimera to align atoms contained in the residues shown. C) Superposition of metal ion ligands in MtIPMS and HCS-lys from *Thermus thermophilus* (TtHCS). PDB files 3u6w (pink) and 2zyf (green) were used for the figure. Here, 3u6w is identical to its representation in panel A. The green sphere in 2zyf represents a Mg^{2+}ion. Residue numbers are shown for both MtIPMS and TtHCS. The site of differential conservation is labeled in red.

[6]. In this enzyme, oxygen atoms from the carbonyl and carboxyl groups of KIV serve as ligands to the divalent cation. Mechanistically, the metal is predicted to help polarize the α-keto group to promote nucleophilic attack by the methyl group from AcCoA. A recent structural report for the catalytic domain of IPMS from *Mycobacterium tuberculosis* (MtIPMS) exhibited alternate coordination architecture for the divalent metal in the absence of substrate [7]. In the absence of KIV, the metal ion is displaced several angstroms and liganded by an asparagine residue (N321 in MtIPMS) in addition to the aspartic acid (D81) and histidine residues (H285/H287) described above (brown structure, Fig. 1A). Upon the addition of KIV to the crystal the metal transitions back to the canonical coordination.

Recent bioinformatics analysis of the DRE-TIM metallolyase superfamily indicates that this alternate metal binding architecture is conserved at the superfamily level, suggesting that it may play a role in catalysis or structural stability [8]. With the exception of homocitrate synthase sequences predicted to be involved in L-lysine biosynthesis (HCS-lys), the asparagine (or glutamine in the case of pyruvate carboxylase) residue acting as an additional ligand to the metal is found in a structurally similar position (Fig. 1B) and is one of a small number of residues strongly conserved throughout the DRE-TIM metallolyase superfamily (Figure S1). An alternate metal coordination architecture similar to that identified in MtIPMS has also been structurally documented in DRE-TIM metallolyase superfamily member HMG-CoA lyase [9]. Conservation of this asparagine at the superfamily level suggests that it may play an important role.

Interestingly, fungal and euglena HCS enzymes in the α-aminoadipate pathway for the biosynthesis of L-lysine are the exception within the superfamily. HCS catalyzes an identical reaction to IPMS using α-ketoglutarate instead of KIV as the α-keto acid substrate. This reaction is the first step in the biosynthesis of L-lysine (HCS-lys) in fungal and euglena organisms and in the production of homocitrate for the nitrogenase cofactor in nitrogen-fixing organisms (HCS-NifV). As identified by the protein similarity network, sequences predicted to be HCS-NifV enzymes contain the conserved asparagine residue, suggesting that the alternate metal binding site is present [8]. In contrast, HCS-lys enzymes contain a differentially conserved isoleucine in place of the conserved asparagine residue. Isoleucine is not capable of coordinating the metal ion suggesting that the alternate metal coordination site is not accessible to these enzymes. The N → I substitution is accompanied by a glutamic acid in place of the conserved aspartic acid, with the glutamic acid acting as a ligand to the divalent cation (green structure, Fig. 1C). The lack of this site in fungal HCS enzymes suggests that the ligand is not essential to the catalytic function of the scaffold or may play a role in additional functionality not required by HCS-lys enzymes.

In order to investigate the catalytic necessity of the alternate metal ion site, site-directed mutagenesis has been employed to create enzyme variants at the conserved aspartic acid and asparagine positions. The resulting enzyme variants have been characterized with respect to KIV-dependent isopropylmalate formation, AcCoA hydrolysis activity, and the ability of Mg^{2+} to inhibit hydrolysis. Overall, the results are consistent with a requirement for the conserved asparagine residue in the condensation activity of MtIPMS. Additionally, variants of MtIPMS that mimic the active site of HCS-lys do not catalyze the condensation reaction.

2. Materials and methods

2.1. Materials

For the site-directed mutagenesis of the MtIPMS gene, oligonucleotides from Eurofins MWG Operon were acquired (Huntsville, AL and Louisville, KY). 4,4′-Dithiopyridine (DTP) was purchased from Acros Organics. Acetyl CoA (AcCoA) and α-ketoisolvalerate (α-KIV) were purchased from Sigma-Aldrich. All other buffers and reagents were of the highest purity grade available and were acquired from VWR International, LLC. The QuikChange Lightning Site-Directed Mutagenesis Kit was obtained from Stratagene. XL Gold cells were purchased from Stratagene, and competent *Escherichia coli* BL21(DE3)pLysS cells were

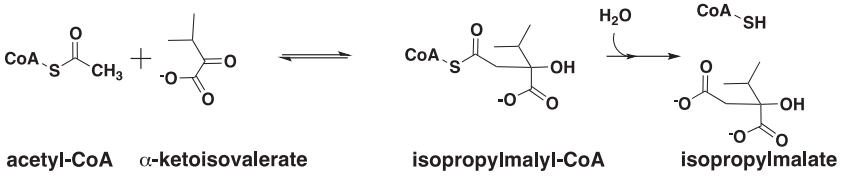

Scheme 1. Reaction catalyzed by IPMS..

purchased from Novagen. The Plasmid DNA Mini Kit I was acquired from Omega. The HisTrap HP column was obtained from GE Healthcare.

2.2. Construction of enzyme variant-containing plasmids

Point mutations were created in the pET28b::LeuA plasmid using the QuikChange Lightning Site-Directed Mutagenesis Kit. The primers used are listed in Table S1. The DNA products were sequenced by Operon to confirm the existence of the desired mutation.

2.3. Expression and purification of enzyme variants

Enzymes were recombinantly expressed in autoinduction media as previously described [10]. Briefly, the plasmids were transformed into *E. coli* BL21(DE3)pLysS cells. The *E. coli* BL21(DE3)pLysS cells were inoculated into 25 mL of LB (30 μg/mL kanamycin, 35 μg/mL chloramphenicol, 0.5% glucose). The cells were then grown at 37 °C for 12–16 h. Approximately 12.5 mL of the overnight culture was added to 400 mL of autoinduction media and grown at 25 °C for 24–36 h. Once the overnight culture reached an OD_{600} of 10 to 15, the cells were isolated by centrifugation (6340 *g*, 4 °C, 10 min). The cell pellet was stored at −80 °C. The cell pellet was resuspended in lysis buffer (20 mM TEA (pH 7.8), 300 mM KCl, 50 mM imidazole). 1 mM of phenylmethanesulfonylfluoride (PMSF) protease inhibitor, DNaseI, 0.25 mg/mL of lysozyme, and $MgCl_2$ were added to the lysis buffer for a total volume of 50 mL. As previously described, the cells were lysed by sonication for 10 min (2.5 min on, 2.5 min off, repeat four times) (Branson Sonifier). The supernatant was retrieved after centrifugation (34,540 *g*, 4 °C, 30 min) and loaded onto a 5 mL HisTrap HP column. The protein was eluted with a linear gradient of 0–250 mM imidazole over 20 to 30 column volumes. An SDS-PAGE gel was run to check the protein purity, and the fractions containing purified enzyme were pooled. The protein was then concentrated to a final volume of approximately 10 mL using an Amicon ultrafiltration apparatus (MWCO of 30 kDa). After treatment with 2 mM EDTA and 1 mM DTT (4 °C, 30 min), the protein was dialyzed three times against 1 L of 20 mM TEA (pH 7.8) for four hours. The purified protein was stored in 10% glycerol at −20 °C. Results from atomic absorption spectroscopy in Chelex-treated 20 mM TEA (pH 7.8), 50 mM KCl buffer indicate that the final enzyme preparation contains ~0.1 equivalents of magnesium.

2.4. Enzymatic assays

Initial velocities for the kinetic assays were determined by following the formation of CoA using 4,4′-dithiopyridine (DTP) at 324 nm ($\varepsilon = 19.8\ mM^{-1}\ cm^{-1}$). A standard reaction mixture contained 50 mM potassium phosphate buffer (pH 7.5), 12 mM $MgCl_2$, 10 μM DTP, and varying concentrations of AcCoA or KIV. Each reaction was initiated by the addition of 10 to 20 nM of the enzyme. Hydrolysis activity was determined using similar conditions in the absence of KIV. Metal-inhibition assays were performed under similar conditions with a range of magnesium chloride concentrations (0–120 mM). The effect of EDTA on AcCoA hydrolysis was determined by the addition of 1 mM EDTA to the reaction conditions described above. All reactions were performed at 25 °C maintained by a circulating water bath.

2.5. Size exclusion chromatography

A GL Superdex 200 10/300 column was equilibrated with 20 mM TEA (pH 7.8) and 100 mM KCl at a flow rate of 0.25 mL/min. The column was calibrated using a molecular weight standard kit (BioRad). After calibration, 100 μL of each enzyme (1 mg/mL concentration) was injected onto the column.

2.6. Data analysis

Steady-state kinetic parameters for AcCoA hydrolysis reactions were determined by a fit of the initial velocities at varying substrate concentrations to the Michaelis–Menten equation (Eq. 1). Here, v is the initial velocity, E_t is the total concentration of enzyme in the reaction, k_{cat} is the maximal velocity of the reaction, K_M is the Michaelis constant for the varied substrate, and [S] is the concentration of the varied substrate.

$$\frac{v}{[E_t]} = \frac{k_{cat} * [S]}{K_M + [S]}. \quad (1)$$

IC_{50} values for metal inhibition of AcCoA hydrolysis were determined by fitting the initial velocities obtained at varying concentrations of magnesium chloride to Eq. 2. Here, v is the initial velocity, v_0 is the initial velocity in the absence of inhibitor, I is the concentration of metal ion, IC_{50} is the concentration of inhibitor that gives 50% inhibition, and n_H is the Hill coefficient.

$$v = v_0 / \left[1 + ([I]/IC_{50})^{n_H}\right]. \quad (2)$$

Approximate molecular weights for the IPMS variants were determined from size exclusion chromatography results. The data was analyzed by plotting the log MW of each standard protein versus the calculated K_{av} partition coefficient value for protein MW standards to create a standard curve, which was then used to calculate molecular weight values for the IPMS variants.

2.7. Multiple sequence alignment for representative DRE-TIM metallolyase superfamily members

A structure-based sequence alignment was created using the Needleman–Wunsch algorithm [11] as implemented with the Matchmaker [12] program in Chimera [13] using the HMGL-like catalytic domains for four representative members of the DRE-TIM metallolyase superfamily: MtIPMS (PDB ID: 3u6w [7]), pyruvate carboxylase from *Rhizobium etli* (PDB ID: 4jx5 [14]), 4-hydroxy-2-ketovalerate aldolase from *Pseudomonas* sp. CF600 (PDB ID: 1nvm [15]), and 3-hydroxy-3-methylglutaryl CoA lyase from *Homo sapiens* (PDB ID: 3mp3 [16]). This alignment was used as a seed to generate the full alignment of representative sequences using MAFFT version 7 [17].

3. Results

3.1. Kinetic parameters of AcCoA hydrolysis

Overall, five enzyme variants were constructed: D81 was substituted with alanine [8] and glutamic acid, N321 was substituted with alanine and isoleucine, and the double substitution D81E/N321I was created to mimic the active site of HCS-lys enzymes. All five enzymes were successfully expressed and purified as described above. None of the enzyme variants were capable of catalyzing KIV-dependent isopropylmalate formation. Size-exclusion chromatography results indicate native molecular weights of 152–178 kDa for the variant enzymes in comparison to the native molecular weight of 171 kDa for wild type MtIPMS (Table S2). The calculated molecular weight for monomeric MtIPMS is approximately 72 kDa. These results suggest that amino acid substitution has not disrupted the dimeric nature of the enzyme. Circular dichroism spectroscopy was also used to compare secondary structure content for the variants with the wild-type enzyme (Figure S2). Spectra from the variants overlaid well with the spectrum for wild-type enzyme suggesting that amino acid substitutions have not significantly disrupted secondary structure elements. Initial attempts to determine kinetic parameters for the variants using the thiol-capture assay (which detects the production of CoA using dithiodipyridine) were complicated when increases in KIV

concentration slowed the rate of reaction. Maximal rates of CoA formation were seen in the absence of KIV, suggesting KIV was not involved in the formation of CoA and instead the variants catalyze the hydrolysis of AcCoA. This activity has been previously reported to occur in wild-type MtIPMS in the absence of KIV [18]. For wild-type MtIPMS, when KIV is present no uncoupled hydrolysis of AcCoA is detected. The enzyme variants display Michaelis–Menten kinetics (Figure S3) with respect to the AcCoA-dependent hydrolysis reaction and the kinetic parameters determined for each enzyme are shown in Table 1. The K_{AcCoA} values are approximately 5–10-fold larger compared for the K_{AcCoA} value determined in the KIV-dependent condensation reaction.

3.2. Metal inhibition of enzyme catalyzed AcCoA hydrolysis

While attempting to identify conditions for maximal rates of AcCoA hydrolysis, an observation was made that decreasing concentrations of the divalent cation (essential for KIV-dependent condensation activity) lead to higher rates of hydrolysis. A systematic approach was taken to evaluate the effect of magnesium chloride concentration on the hydrolysis activity of the enzyme variants. As can be seen in Fig. 2, hydrolysis activity of wild-type and two enzyme variants is inhibited by increasing concentrations of magnesium chloride with IC_{50} values in the low millimolar range (Table 2). The lack of requirement for the metal ion in the AcCoA hydrolysis reaction was confirmed by the addition of 1 mM EDTA to an assay for wild-type MtIPMS; this had no effect on the rate of the reaction. Three of the enzyme variants (D81A, N321I, and D81E/N321I) were insensitive to increases in magnesium chloride concentration up to 50 mM. Proteolytic removal of the *N*-terminal $(His)_6$-tag did not affect the metal inhibition parameters for wild-type MtIPMS, ruling out a contribution from this additional divalent metal binding site (Figure S4).

4. Discussion

Analysis of enzyme superfamilies containing diverse functionalities can allow for the identification of common catalytic strategies. In the case of the DRE-TIM metallolyase superfamily, members are proposed to stabilize a common enolate intermediate using a conserved active site arginine residue. All members of the superfamily also require a divalent cation for full activity; however, the exact role of the metal ion in catalysis is not clear for this superfamily. The recent structural and bioinformatics results indicate the presence of an alternate metal architecture using a conserved asparagine residue to act as an additional ligand to the metal ion.

4.1. D81 and N321 are critical to MtIPMS function

MtIPMS variants with substitutions at the asparagine and aspartic acid positions are inactive with respect to the KIV-dependent isopropylmalate formation reaction suggesting that these residues are important in catalysis or for structural integrity. Combined results from size-exclusion chromatography and circular dichroism spectroscopy suggest that the substitutions have not grossly affected the structure of the enzyme, ruling out a large-scale structural perturbation in the inactivity of the variants. The D81A substitution has previously been shown to be inactive, most likely due to the disruption of the metal binding site [8]. Here, the D81E substitution retains a side chain capable of acting as a ligand (as shown by HCS sequences), but IPMS activity is not rescued. Substitutions at N321 also abolish IPMS activity. The N321 side chain is ~3 Å from the side chain of D81 in both metal architectures of MtIPMS (and in other superfamily members). Thus, one explanation for the results is that N321 may be responsible for proper orientation of D81 in catalysis, however further structural studies are required to test this hypothesis.

Table 1
Kinetic parameters for AcCoA hydrolysis for wild-type MtIPMS and variants.

MtIPMS variant	k_{cat} (min^{-1})	K_{AcCoA} (μM)
WT	19 ± 2	253 ± 48
D81A	3 ± 1	97 ± 13
D81E	7 ± 1	233 ± 40
N321A	9 ± 1	123 ± 4
N321I	9 ± 1	262 ± 55
D81E/N321I	8 ± 1	163 ± 28

4.2. AcCoA hydrolysis is not affected by the substitution of D81 or N321

All of the enzyme variants were capable of catalyzing the hydrolysis of AcCoA in the absence of KIV. The catalytic machinery necessary for hydrolysis in the isopropylmalate formation reaction or the AcCoA hydrolysis reaction has yet to be identified. Normal solvent kinetic isotope effects are measured when pyruvate is used as an alternate substrate for MtIPMS ruling out a metal-promoted water molecule in the IPMS reaction, suggesting the involvement of side chains in the active site [18]. Consistent with this hypothesis, the AcCoA hydrolysis reaction catalyzed by the MtIPMS variants was determined to be independent of exogenous magnesium and insensitive to the addition of EDTA. Surprisingly, in wild-type, D81E, and N321A MtIPMS, AcCoA hydrolysis activity is inhibited by the addition of magnesium chloride, with apparent IC_{50} values of 5, 9, and 3 mM, respectively (Fig. 2). This is in stark contrast to the absolute requirement for a divalent ion in the isopropylmalate formation reaction [19]. The addition of magnesium did not affect AcCoA hydrolysis in the remaining enzyme variants (D81A, N231I, and D81E/N321I), suggesting that these substitutions have altered the ability of the metal to interact with the enzyme.

One possible explanation for these results is that metal at the canonical (Asp/Glu)/HXH site is responsible for the inhibition of AcCoA hydrolysis. While not a direct measurement of metal affinity, IC_{50} values determined for metal ions in the AcCoA hydrolysis reaction with wild-type and variant MtIPMS enzymes are identical to the K_{act} value (concentration of magnesium resulting in 50% activation) determined for magnesium in the condensation reaction with wild-type MtIPMS. [19] Thus, the susceptibility of AcCoA hydrolysis to metal inhibition in D81E and N321A MtIPMS suggests that the site of metal-inhibition, presumably the primary (Asp/Glu)/HXH metal binding site, is unperturbed in these enzyme variants.

4.3. MtIPMS cannot use HCS-like active site architecture

If the evolutionarily conserved asparagine is critical for catalysis, it is of interest to understand why HCS-lys enzymes can catalyze a similar reaction while lacking the alternate metal binding site. As described above, fungal HCS enzymes have a pair of conserved substitutions with a D → E substitution for the metal binding carboxylate. In order to accommodate the extra methylene group from glutamic acid, HCS-lys enzymes have a conserved compensatory substitution of the smaller isoleucine at the N321 position. The doubly substituted D81E/N321I MtIPMS is unable to support isopropylmalate formation activity, and $MgCl_2$ does not inhibit the enzyme's hydrolysis activity. One explanation for this result is that additional changes to the active site are required for MtIPMS to be active in the absence of the alternate metal binding site. However, closer inspection of the active site architecture for the two enzymes shows no readily apparent changes that could be proposed.

An alternate explanation rooted in the superfamily-based evolution is that HCS activity in the absence of the alternate metal binding site is due to different functional properties of the two enzymes. Indeed biochemical characterization of MtIPMS and HCS from *Saccharomyces cerevisiae* (ScHCS) indicates several functional differences. Most striking is the difference in regulatory properties between the two enzymes. MtIPMS, which is feedback inhibited by L-leucine, contains a *C*-

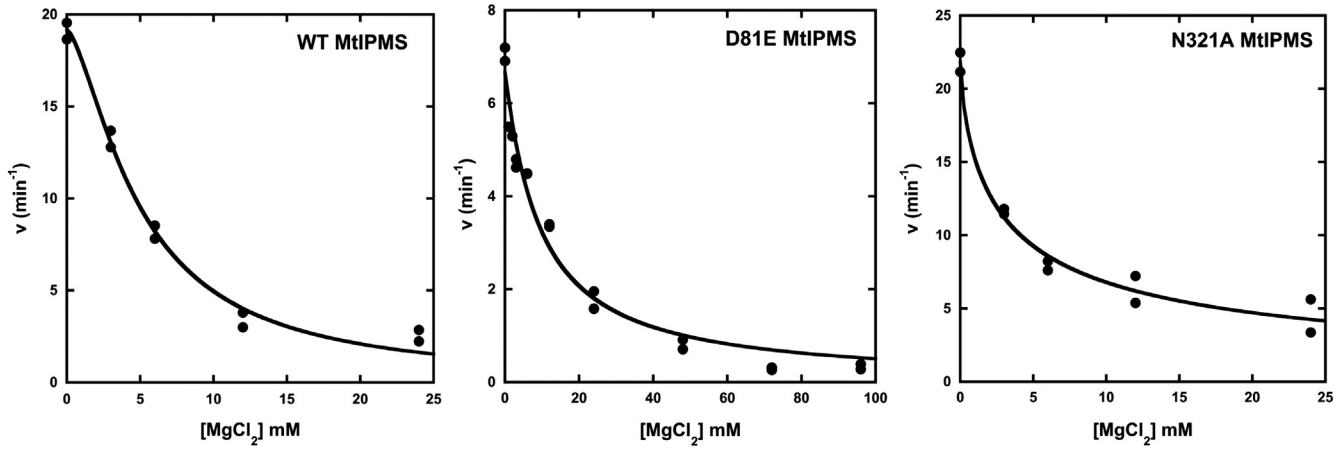

Fig. 2. Inhibition of AcCoA hydrolysis by $MgCl_2$ for wildtype and variant MtIPMS. Experimental conditions are as described in Materials and methods. The solid line is from a fit of the data to Eq. 2.

terminal regulatory domain and is inhibited allosterically. In contrast ScHCS, which is feedback inhibited by L-lysine, is subject to competitive inhibition [20]. Mutational studies also suggest differences in the identity of conserved residues responsible for acid–base chemistry. Alanine substitutions for active site residues H379 and E218 (MtIPMS numbering) cause either loss of or significant decreases in HCS activity [21] while identical substitutions in MtIPMS result in only 4-to-30-fold decreases in activity [22].

5. Conclusions

Overall, the results are consistent with the asparagine residue responsible for the alternate metal architecture in MtIPMS being required for full catalytic activity. One possible explanation for this result is that N321 is responsible for properly orienting D81 in the active site, though future structural studies are required to test this hypothesis. The ability of N321A MtIPMS to catalyze AcCoA hydrolysis with kinetic parameters similar to the wild-type enzyme suggests that the adjacent site is not involved in the hydrolytic step following the condensation reaction. Finally, due to the superfamily level of conservation, it will be of interest to determine if this site is critical for activity in other superfamily members.

Acknowledgements

This work was supported by NSF grant MCB-1254077 (P.A.F.). Molecular graphics and analyses were performed with the UCSF Chimera package. Chimera is developed by the Resource for Biocomputing, Visualization, and Informatics at the University of California, San Francisco (supported by NIGMS P41-GM103311). We thank Dr. Holly Ellis (Auburn University) for her assistance in circular dichroism spectroscopy.

Table 2
Apparent inhibition constants determined for the inhibition of AcCoA hydrolysis by divalent metal for wild-type MtIPMS and variants[a].

MtIPMS variant	IC_{50} (mM)
WT	5 ± 1
D81A	–[b]
D81E	9 ± 1
N321A	3 ± 1
N321I	–
D81E/N321I	–

[a] Experimental conditions described in Materials and methods.
[b] No inhibition observed up to 50 mM.

Appendix A. Supplementary data

Supplementary data to this article can be found online at http://dx.doi.org/10.1016/j.bbapap.2014.07.013.

References

[1] J.A. Gerlt, P.C. Babbitt, M.P. Jacobson, S.C. Almo, Divergent evolution in enolase superfamily: strategies for assigning functions, J. Biol. Chem. 287 (2012) 29–34.
[2] K.N. Allen, D. Dunaway-Mariano, Markers of fitness in a successful enzyme superfamily, Curr. Opin. Struct. Biol. 19 (2009) 658–665.
[3] M.A. Hicks, A.E. Barber 2nd, L.A. Giddings, J. Caldwell, S.E. O'Connor, P.C. Babbitt, The evolution of function in strictosidine synthase-like proteins, Proteins 79 (2011) 3082–3098.
[4] J.A. Gerlt, P.C. Babbitt, Divergent evolution of enzymatic function: mechanistically diverse superfamilies and functionally distinct suprafamilies, Annu. Rev. Biochem. 70 (2001) 209–246.
[5] F. Forouhar, M. Hussain, R. Farid, J. Benach, M. Abashidze, W.C. Edstrom, S.M. Vorobiev, R. Xiao, T.B. Acton, Z. Fu, J.J. Kim, H.M. Miziorko, G.T. Montelione, J.F. Hunt, Crystal structures of two bacterial 3-hydroxy-3-methylglutaryl-CoA lyases suggest a common catalytic mechanism among a family of TIM barrel metalloenzymes cleaving carbon–carbon bonds, J. Biol. Chem. 281 (2006) 7533–7545.
[6] P.A. Frantom, Structural and functional characterization of alpha-isopropylmalate synthase and citramalate synthase, members of the LeuA dimer superfamily, Arch. Biochem. Biophys. 519 (2012) 202–209.
[7] F.H. Huisman, N. Koon, E.M. Bulloch, H.M. Baker, E.N. Baker, C.J. Squire, E.J. Parker, Removal of the C-terminal regulatory domain of alpha-isopropylmalate synthase disrupts functional substrate binding, Biochemistry 51 (2012) 2289–2297.
[8] A.K. Casey, H., M. A., J.L. Johnson, P.C. Babbitt, P.A. Frantom, Mechanistic and bioinformatic investigation of a conserved active site helix in alpha-isopropylmalate synthase form *Mycobacterium tuberculosis*, a member of the DRE-TIM metallolyase superfamily, Biochemistry 53 (2014) 2915–2925.
[9] Z. Fu, J.A. Runquist, F. Forouhar, M. Hussain, J.F. Hunt, H.M. Miziorko, J.J. Kim, Crystal structure of human 3-hydroxy-3-methylglutaryl-CoA Lyase: insights into catalysis and the molecular basis for hydroxymethylglutaric aciduria, J. Biol. Chem. 281 (2006) 7526–7532.
[10] A.K. Casey, J. Baugh, P.A. Frantom, The slow-onset nature of allosteric inhibition in alpha-isopropylmalate synthase from Mycobacterium tuberculosis is mediated by a flexible loop, Biochemistry 51 (2012) 4773–4775.
[11] S.B. Needleman, C.D. Wunsch, A general method applicable to the search for similarities in the amino acid sequence of two proteins, J. Mol. Biol. 48 (1970) 443–453.
[12] E.C. Meng, E.F. Pettersen, G.S. Couch, C.C. Huang, T.E. Ferrin, Tools for integrated sequence-structure analysis with UCSF Chimera, BMC Bioinforma. 7 (2006) 339.
[13] Z. Yang, K. Lasker, D. Schneidman-Duhovny, B. Webb, C.C. Huang, E.F. Pettersen, T.D. Goddard, E.C. Meng, A. Sali, T.E. Ferrin, UCSF Chimera, MODELLER, and IMP: an integrated modeling system, J. Struct. Biol. 179 (2012) 269–278.
[14] A.D. Lietzan, M. St Maurice, Insights into the carboxyltransferase reaction of pyruvate carboxylase from the structures of bound product and intermediate analogs, Biochem. Biophys. Res. Commun. 441 (2013) 377–382.
[15] B.A. Manjasetty, J. Powlowski, A. Vrielink, Crystal structure of a bifunctional aldolase–dehydrogenase: sequestering a reactive and volatile intermediate, Proc. Natl. Acad. Sci. U. S. A. 100 (2003) 6992–6997.
[16] Z. Fu, J.A. Runquist, C. Montgomery, H.M. Miziorko, J.J. Kim, Functional insights into human HMG-CoA lyase from structures of Acyl-CoA-containing ternary complexes, J. Biol. Chem. 285 (2010) 26341–26349.

[17] K. Katoh, D.M. Standley, MAFFT multiple sequence alignment software version 7: improvements in performance and usability, Mol. Biol. Evol. 30 (2013) 772–780.
[18] L.P. de Carvalho, J.S. Blanchard, Kinetic and chemical mechanism of alpha-isopropylmalate synthase from *Mycobacterium tuberculosis*, Biochemistry 45 (2006) 8988–8999.
[19] L.P. de Carvalho, J.S. Blanchard, Kinetic analysis of the effects of monovalent cations and divalent metals on the activity of *Mycobacterium tuberculosis* alpha-isopropylmalate synthase, Arch. Biochem. Biophys. 451 (2006) 141–148.
[20] B. Andi, A.H. West, P.F. Cook, Regulatory mechanism of histidine-tagged homocitrate synthase from *Saccharomyces cerevisiae*. I. Kinetic studies, J. Biol. Chem. 280 (2005) 31624–31632.
[21] J. Qian, J. Khandogin, A.H. West, P.F. Cook, Evidence for a catalytic dyad in the active site of homocitrate synthase from *Saccharomyces cerevisiae*, Biochemistry 47 (2008) 6851–6858.
[22] L.P. de Carvalho, P.A. Frantom, A. Argyrou, J.S. Blanchard, Kinetic evidence for interdomain communication in the allosteric regulation of alpha-isopropylmalate synthase from *Mycobacterium tuberculosis*, Biochemistry 48 (2009) 1996–2004.